Free Radical Biology and Medicine 84 (2015) 373–384

Contents lists available at ScienceDirect

Free Radical Biology and Medicine

journal homepage: www.elsevier.com/locate/freeradbiomed

Original Contribution

Retinal damage induced by commercial light emitting diodes (LEDs)

Imene Jaadane [a], Pierre Boulenguez [b], Sabine Chahory [c], Samuel Carré [b], Michèle Savoldelli [a], Laurent Jonet [a], Francine Behar-Cohen [a,d], Christophe Martinsons [b], Alicia Torriglia [a,*]

[a] INSERM U1138, Centre de Recherches des Cordeliers, Université Paris Descartes, Université Pierre et Marie Curie, Paris, France
[b] CSTB, Centre Scientifique et Technique du Bâtiment, Division Eclairage et électromagnétisme, Saint Martin d'Heres, France
[c] ENVA, Ecole Nationale Vétérinaire d'Alfort, Maison Alfort, France
[d] Hôpital Ophtalmique Jules Gonin, Lausanne, Switzerland

ARTICLE INFO

Article history:
Received 3 December 2014
Received in revised form
26 March 2015
Accepted 27 March 2015
Available online 8 April 2015

Keywords:
LED
Retinal degeneration
Apoptosis
Necrosis
Necroptosis
Stress response
Oxidative stress
Blue light
Wavelength

ABSTRACT

Spectra of "white LEDs" are characterized by an intense emission in the blue region of the visible spectrum, absent in daylight spectra. This blue component and the high intensity of emission are the main sources of concern about the health risks of LEDs with respect to their toxicity to the eye and the retina. The aim of our study was to elucidate the role of blue light from LEDs in retinal damage. Commercially available white LEDs and four different blue LEDs (507, 473, 467, and 449 nm) were used for exposure experiments on Wistar rats. Immunohistochemical stain, transmission electron microscopy, and Western blot were used to exam the retinas. We evaluated LED-induced retinal cell damage by studying oxidative stress, stress response pathways, and the identification of cell death pathways. LED light caused a state of suffering of the retina with oxidative damage and retinal injury. We observed a loss of photoreceptors and the activation of caspase-independent apoptosis, necroptosis, and necrosis. A wavelength dependence of the effects was observed. Phototoxicity of LEDs on the retina is characterized by a strong damage of photoreceptors and by the induction of necrosis.

Introduction

Retinal degenerations, whether genetic or not, involve death of photoreceptors. Environmental factors such as smoking, obesity, and hypertension are important in the progression of the different retinopathies [1]. In addition, the exposure to intense natural or artificial light can be detrimental to eye tissues by causing photochemical damages. Many studies have been conducted to evaluate the effect of light on the evolution of preexisting retinopathy [2]. For the last few years this interest has been concentrated on age-related macular degeneration (AMD), a leading pathology of the elderly in Western countries [3]. After many conflicting studies it was concluded that light is a risk factor in the early stages of AMD, although it is not recognized as an aggravating factor for the pathology [4–6].

The retinal damages induced by light depend on radiation intensity, radiation wavelength, and time of exposure [7,8]. Light-induced retinal lesions are characterized by a degeneration of photoreceptors outer segments leading to their death by apoptosis [9,10].

Recently, the use of new technologies in domestic lighting induced a renewal of the interest on the effects of light on the retina. Among these new devices, light emitting diodes (LEDs) are at the center of this interest. From a technical point of view LEDs have many advantages such as low energy consumption, high mechanical strength, and, especially, long life. One of the major concerns with the use of this technology is the emission spectrum of LEDs. The spectrum of LEDs is characterized by an intense blue light component absent in the daylight spectra [11]. In recent years, governmental agencies such as the ANSES (French Agency for Food, Environmental and Occupational Health and Safety) in 2010 stressed the need for extensive experimental studies on the phototoxicity of LEDs to confirm or refute the fears raised by researchers, ophthalmologists, and physicists concerning the intensive use of these devices. Actually, the most commonly used LEDs present a high luminance level and generate a visual discomfort related to the "punctual" character of the emitting surfaces. In addition, the spectral imbalance of white LEDs available on the market, due to the production of white light by the processing of a high-frequency radiation and reemission in a complementary wavelength, exposes the eye to residual short wavelength

* Correspondence to: INSERM U1138, Centre de Recherches des Cordeliers, 15, rue de l'école de Médecine, 75006, Paris, France.
E-mail address: alicia.torriglia@inserm.fr (A. Torriglia).

http://dx.doi.org/10.1016/j.freeradbiomed.2015.03.034
0891-5849/

radiations, the most dangerous to the retina. This problem could be increased by a reduction of the pupillary contraction, stimulated at around 480 nm, a region of low emission in the spectrum of some LEDs, resulting in an increase of retinal light exposure.

In this study, we investigate, in rats, the molecular mechanism of retinal degeneration by using five different LEDs: white LEDs, green LEDs (507 nm), and three blue LEDs (449, 467, 473 nm) to evaluate the role of blue radiation in cellular damage and the progression of retinal lesions.

Materials and methods

Animals

Six-week-old male Wistar rats were purchased from Janvier labs and kept 1 week for adaptation in our animal facilities in a light cycle of 12 h. All procedures were in compliance with the animal use and care committee of the National Veterinary School of Alfort.

Light source

We used two types of lighting devices built and characterized by the Lighting and Electromagnetism Division of the Scientific and Technical Center for Building (CSTB, Saint Martin d'Heres, France): the first contains only white LEDs (Xanlite XXX Evolution 5 W). The second device has four types of LEDs with different wavelengths in the blue region of the spectrum: green LEDs (507 nm) and three blue LEDs (449, 467, 473 nm) (Table 1). Both devices possess a diffuser improving the directional uniformity of the radiation. The spectral distributions and intensities of light sources were established and tested by the CSTB. The spectra of emission of the different devices are shown on Supplementary Fig. 1. The construction of the blue device is seen in Supplementary Fig. 2. Dose of exposure was calculated by using dedicated software developed by the CSTB for these sets of experiments. The calculations relied on *in situ* spectrophotometric measurements and on a model of the Wistar rat vision and behavior. For each type of source, spectral irradiance and uniformity were measured using a fiber optic spectrophotometer with a diffusing head (Ocean Optics-R2000+). In the lighting device only the ceiling of the cage was emitting light. Thus, at a given instant, retinal dose of a freely moving rat depended on his head posture. For the overall dose it was estimated that, on average, a rat keeps his head aligned with his body. Following the arguments given in the review article [12], the eye of a rat was modeled as a hemisphere. All the formalism used is described in supplementary information 1.

Light exposure

Wistar rats were kept in transparent cages placed under the light sources suspended 25 cm above the top of cages. The rats were exposed to a constant light for 6, 12, 18, 24, 48, and 72 h, without been previously dark-adapted. After illumination, the rats were sacrificed using sodium pentobarbital (Ceva, La Ballastiere, France) at lethal dose by intraperitoneal injection. Their eyes were immediately enucleated and fresh-frozen in optical cutting temperature compound (Tissue Tek compound Sakura) using liquid nitrogen and stored at −80 °C until sectioning. The 10 μm cryosections were prepared by using a cryostat (Leica CM 3050S) and stored at −20 °C until immunohistochemical analysis. Alternatively, for biochemical experiments, neuroretina was dissected and frozen immediately at −20 °C.

Table 1
Physical parameters of used LEDs.

LED name	Wavelengths (nm)	Luminance ($cd.m^{-2}$)	Radiance ($W.m^{-2}.sr^{-1}$)
White LED Xanlite XXX evolution	460–600	2680	8.33
Nichia NCSE119A blue-green	507	643	1.81
Cree XP-E blue	473	268	2.49
Nichia NCSB119 blue	467	234	3.1
Cree XP-E royal blue	449	102	2.82

Cd, candela; W, watt; sr, steradian.

Dilated fundus examination

After the exposure rats were examined by Dr. S. Chahory (ophthalmological veterinary) using a 28D lens (Heine Optotechnik Herrsching, Germany).

Intravitreal injection of propidium iodide (PI)

After light exposure, the rats were anesthetized by an intraperitoneal injection of sodium pentobarbital at 25 mg/kg. A local anesthesia was performed by an instillation of Tetracaine 1% (Faure, Novartis Pharma). The intravitreal injection of propidium iodide (Sigma Aldrich, Saint-Quentin Fallavier, France) was carried out under a surgical microscope using a 30 G needle mounted on an insulin syringe (BD Micro-Fine, Becton Dickinson S.A., Le Pont de Claix, France). Propidium iodide was injected at a concentration of 1 μg per eye in a volume of 10 μL of balanced salt solution (BSS, Bausch and Lomb). The rats were sacrificed using sodium pentobarbital (Ceva, La Ballastiere, France) at lethal dose by intraperitoneal injection. Their eyes were immediately enucleated after killing and fixed in 4% paraformaldehyde for 2 h at room temperature, washed several times with PBS, and then embedded in optimal cutting compound for preparation of cryosections.

Protein extraction from light-exposed retinas

After defrosting, the retinas were homogenized in 20% weight–volume of M-PER extraction reagent (Thermo Scientific, Illkirch, France), using a pellet pestle motor homogenizer (Kontes) on an ice bed. The homogenate was then incubated on ice for 15 min and centrifuged (15,000 *g*, 4 °C) for 15 min. Supernatant was recovered for Western blot analysis.

Western blot

After extraction of retinal proteins, their amount was measured with the bicinchoninic acid (BCA) protein assay kit (Thermo Scientific, Illkirch, France), according to the manufacturer's instructions. Bovine serum albumin (BSA) was used as standard. Laemmli sample buffer was added for Western blot analysis. Extracted proteins were separated in a 12% SDS-PAGE, immobilized on nitrocellulose membrane (Protan, Whatman, GE Healthcare, Versailles, France), and blotted with specific primary antibody at 1/1000 dilution: anti-PKC zeta (Santa Cruz sc-216, Clinisciences, Nanterre, France), anti-phospho-PKC zeta (Santa Cruz sc-12894R, Clinisciences, Nanterre, France), anti-actin (Santa Cruz sc-1616, Clinisciences, Nanterre, France), anti-LEI/L-DNase II (produced in our laboratory) [13]. The secondary antibodies conjugated to HRP (Vector, Eurobio, Les Ulis, France) were used in a 1/5000 dilution. Finally, Luminata Forte Western HRP substrate (Millipore, Merck Chimie, Fontenay sous Bois, France) was used to reveal the signal.

Poly-ADP-ribose polymerase (PARP-1) immunoblot

After the eyes were enucleated the retina were extracted, rinsed in PBS, and homogenized in Laemmli sample buffer using a pellet pestle motor (Kontes). Proteins were measured as before, and 40 μg

of protein was loaded on the top of a 10% SDS-PAGE, and transferred to a High-Bound ECL nitrocellulose membrane (Protan, Whatman, GE Healthcare, Versailles, France). PARP-1 was developed using the monoclonal C-2-10 antibody (Biovision, Milpitas, USA) diluted in PBS Tween 0.1% at 1/500 dilution. Development of the labeled bands was done by using a HRP-conjugated secondary antibody and the Luminata Forte Western HRP substrate (Millipore, Eurobio, Les Ulis, France).

Immunohistochemistry

Cryosections of the eyes were washed twice with PBS containing Ca^{2+} and Mg^{2+}, fixed in 4% paraformaldehyde for 15 min at room temperature (all steps were performed at room temperature), and then washed twice with PBS. Permeabilization was performed with 0.3% Triton X-100 for 20 min. Then, the cryosections were washed twice with PBS, and nonspecific protein binding sites were blocked by 1 h incubation in a blocking buffer containing 1% nonfat milk in PBS. Samples were then incubated with specific primary antibodies in 0.1% nonfat milk in PBS diluted at 1/100 for 1 h. A complete list of the antibodies used is shown on Table 2. This was followed by two washes with PBS and incubation for 1 h with a 1/500 dilution of specific secondary antibodies (Invitrogen, Life Technologies, Saint Aubin, France). Samples were washed twice with PBS, incubated for 5 min with 4,6-diaminidino-2-phenyl indoledichloride (DAPI 1/5000) (Sigma Aldrich, Saint-Quentin Fallavier, France), and then washed again three times with PBS. Finally, cryosections were coverslipped with Fluoromount (Sigma, Saint-Quentin Fallavier, France). Immunoreactivity was visualized using fluorescence microscopy with an Olympus microscope BX51 (Olympus France, Rungis, France) or a Zeiss LSM 710 confocal microscope.

Terminal transferase dUTP nick end labeling (TUNEL)

Cryosections were air-dried and fixed in 4% paraformaldehyde 15 min at room temperature and washed twice with PBS. After permeabilization with 0.3% Triton X-100 in PBS for 20 min at room temperature and an additional PBS wash, the TUNEL assay was performed using two different protocols. For the classical protocol, cryosections were incubated with the TUNEL reaction mix (Roche Molecular Biochemical's, Meylan, France) according to the manufacturer's instructions. For the second protocol, the sections were previously incubated for 30 min with calf intestinal alkaline phosphatase 6.66 U/section (Invitrogen, Life Technologies, Saint Aubin, France) at 37 °C. In both cases, the tissues were rinsed three times after TUNEL reaction with PBS and incubated with DAPI 1/5000. Finally, after three washes with PBS, cryosections were coverslipped with fluoromount (Sigma Aldrich, Saint-Quentin Fallavier, France). Immunoreactivity was visualized using an Olympus BX51 fluorescence microscope (Olympus France, Rungis, France) or a Zeiss LSM 710 confocal microscope.

Transmission electron microscopy analysis (TEM)

TEM was performed on nonexposed retinas and on retinas exposed 18 h to the white LEDs. After enucleation the eyes were fixed in 4% glutaraldehyde cacodylate buffer (0.1 M, pH 7.4) for 5 h. Specimens were additionally fixed in 1% osmium tetroxide in cacodylate buffer (0.2 M, pH 7.4) and progressively dehydrated in graduated ethanol solution (50, 70, 95, and 100%) and then in propylene oxide. Each area of interest was separated in four samples, included in epoxy resin, and oriented. Semithin sections (500 nm) were obtained with an ultramicrotome (LEICA Ultracut UCT, Austria) and stained with toluidine blue. Ultrathin sections (60 nm) were contrasted by uranyl acetate and lead citrate and analyzed with a transmission electron microscope (Philips CM10, Netherlands) with a GATAN ES100W camera (USA).

Results

Dilated fundus examination (DFE) showed no bleaching of the retina

DFE is a diagnostic procedure used to evaluate the internal ocular health. Until today, regulations of light toxicity on the retina have established ELV (exposure limit values) [14]. These ELV are based on a study of fundus examination following a single exposure to light for 8 h. They establish that light is toxic to the eye when there is a bleaching of the retina. In our study, DFE was performed just after exposure by a veterinary ophthalmologist and two assistants. No bleaching of the retina was detected in rats exposed for 12 h to 3 days with the different types of LEDs used in this study. However,

Table 2
Antibodies used in experiments.

Antibody	Source	Application	Reference
Actin	Goat	WB	Santa Cruz (sc-1616)
AIF (apoptosis inducing factor E20)	Rabbit	WB/IHC	Abcam
Caspase 8 (p18)	Goat	WB	Santa Cruz
CD11B	Mouse	IHC	Serotec
Cleaved caspase 3 (Asp175)	Rabbit	WB/IHC	Cell Signaling
GFAP	Rabbit	IHC	Dako
8-Hydroxyguanosine (15A3)	Mouse	IHC	Abcam
Iba1	Rabbit	IHC	Cell Signaling
Lamin B	Goat	IHC	Santa Cruz (sc-6216)
LEI/L-DNase II	Rabbit	WB/IHC	Home-made
Nitro-tyrosine (11C2)	Mouse	WB/IHC	Santa Cruz
P62/SQSTM1	Mouse	WB/IHC	Abcam
PARP (C210)	Mouse	WB	BioVision
Phospho-NFkB p65 (S311)	Rabbit	WB/IHC	Abcam (ab-51059)
Phospho-PKC zeta (Thr 410)	Rabbit	WB/IHC	Santa Cruz (sc-12894R)
PKC zeta (C20)	Rabbit	WB/IHC	Santa Cruz
RIP1 (receptor interacting protein)	Mouse	WB/IHC	BD
RIP3 (receptor interacting protein)	Rabbit	WB	Sigma Aldrich

WB, Western blot; IHC: immunohistochemistry.

an important chemosis, indicating an edema of the ocular tissues, was present in almost all the animals during the first 24 h of exposure (Supplementary Fig. 3), disappearing thereafter.

Damages and signs of oxidative stress induced by LEDs

In order to explore photochemical lesions in the retina, we studied inflammation signs that may be associated with chemosis and edema induced by white LED exposure. Semithin sections of retina showed an important interphotoreceptor edema (Supplementary Fig. 4). Immunohistochemistry (IHC) staining of CD11b (integrin αM) and ionized calcium binding adaptor molecule 1 (Iba 1) on retina exposed for 1 and 2 days showed an activation of microglia and macrophage infiltration in the retina revealing retinal inflammation (Fig. 1).

Signs of oxidative stress on DNA/RNA were investigated by 8-hydroxyguanosine (HGN) staining (Fig. 2 and Supplementary Fig. 5). Protein oxidation was assessed by nitro-tyrosine (N-Tyr) staining (Fig. 2, N-Tyr, and Supplementary Fig. 5). The LED-exposed rats presented an increase of HGN immunostaining mostly in the inner nuclear layer (INL) and in the ganglion cell layer of retina exposed for 18 h (125 J/cm^2), although a faint increase in the labeling of the outer nuclear layer (ONL) was also seen. For the same exposure time, N-Tyr immunostaining was higher in all the retina layers compared to rats kept in normal cycling light (NE) (Fig. 2 and Supplementary Fig. 5). However, we found a striking increase of labelling in photoreceptor outer segments (POS) and in photoreceptors inner segments (PIS). Moreover, a closer examination of the ONL showed a radial labeling that was prolonged in some cases to the inner plexiform layer (IPL) and the inner nuclear layer (INL), suggesting a labeling (partial and nonexclusive) of the Müller cells. These results revealed that light emitted from commercially available LEDs induced oxidative damage in the entire retina, at the DNA and protein levels. This damage triggered classical stress responses by increasing the expression of p62 (also called sequestosome) in all the nuclear layers of the retina (Fig. 2, p62). As expected a stress reaction was also seen at the Müller cell level characterized by an increase of the intermediate filament glial fibrillary acid protein (GFAP) (Fig. 2). Interestingly, this response of the Müller cells was quite early, since we saw it after 12 h of exposure (Supplementary Fig. 5, dose: 81 J/cm^2). GFAP, a marker of Müller cells activation [15], was restricted, in normal retina, to the feet of the Muller cells. After 12 h of white LED exposure, increased GFAP immunostaining was detected in the inner limiting membrane. At 18 h (125 J/cm^2), some processes of Müller cells extended from the outer plexiform layer (OPL) to the ganglion cell layer (GCL). Increased GFAP staining was prominent over the entire retina after 24 h (151 J/cm^2) of exposure to white LEDs. These results suggested a reactive gliosis spanning the entire retina following Müller cell activation.

LED-induced retinal degeneration

To investigate whether LED light induced retinal cell death, DAPI staining was used to reveal morphological changes in the nuclei of cells from retina exposed to LEDs compared to unexposed retina (Supplementary Fig. 6). We observed disorganization and a reduced thickness of the ONL. The decrease in ONL thickness was dependent on the time of exposure and it was maximal at 3 days (453 J/cm^2). Note that GNL and INL seemed preserved.

LED-induced retinal cell death

The decrease in ONL thickness indicated retinal degeneration and suggested the presence of cellular demise. In order to investigate this issue a TUNEL assay was used. As seen in Fig. 3A, many apoptotic cells were detected after 18 h of exposure to white LEDs, but apoptotic cells were also detected thereafter (Supplementary Fig. 7), with a maximum at 48 h of exposure (303 J/cm^2).

To study classical apoptosis implications in photoreceptor cell death, we investigated the activation of caspase 3. To do this we used

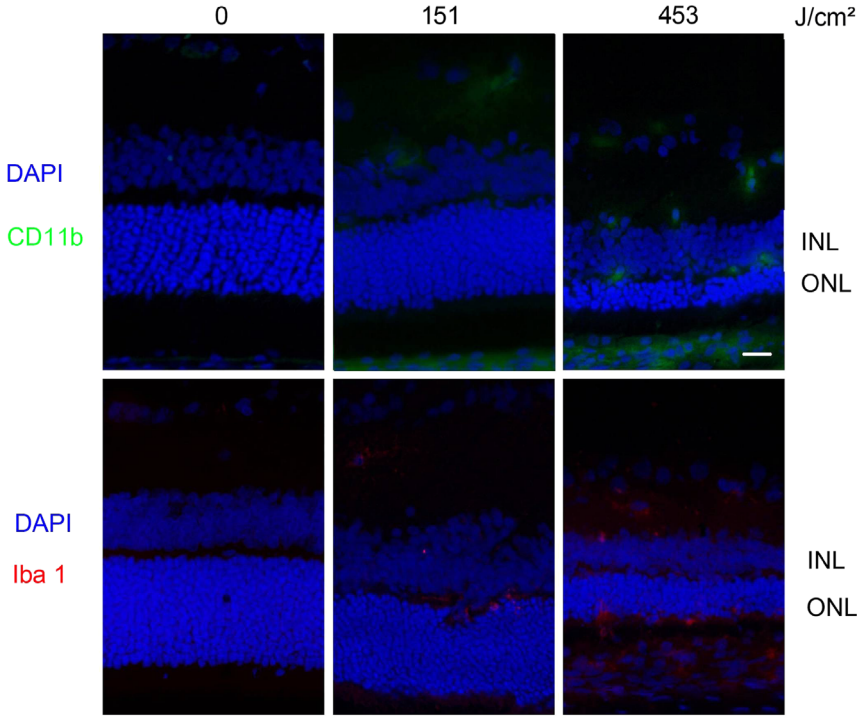

Fig. 1. Inflammatory response after white LED exposure. Male Wistar rats aged 7 weeks ($n=4$) were exposed to Xanlite XXX Evolution 5 W for 1 and 3 days, receiving the estimated retinal dose of light indicated. At the end of the exposure period the eyes were included in optimal cutting temperature medium (Tissue Tek), cryosectioned, and immunostained with anti-CD11b (green) or anti-Iba 1 (red); nuclei were counterstained with DAPI (blue). ONL: outer nuclear layer; INL: inner nuclear layer. Scale bar represents 20 μm.

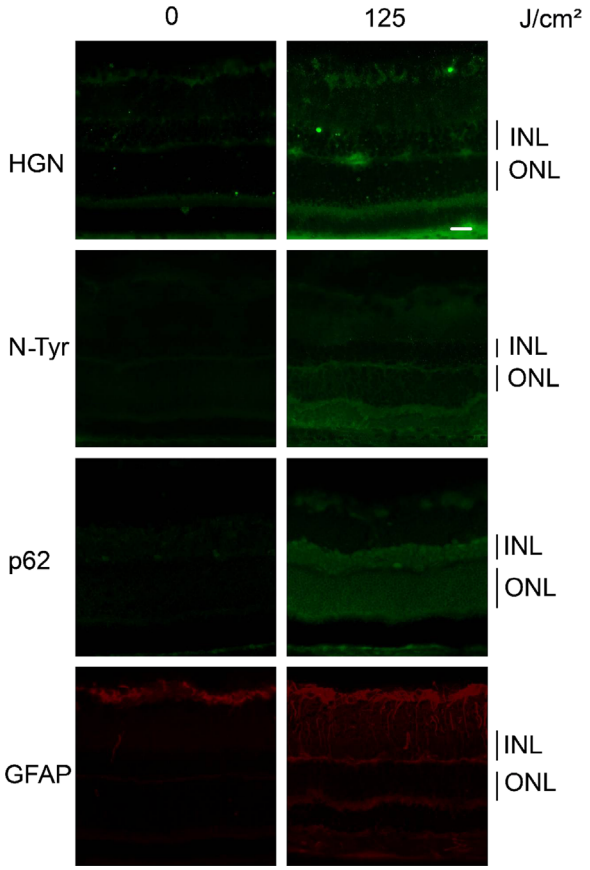

Fig. 2. Oxidative stress response after white LED exposure. Male Wistar rats aged 7 weeks ($n=4$) were exposed to Xanlite XXX Evolution 5 W for 18 h, receiving the estimated retinal dose of light indicated. At the end of the exposure period the eyes were included in optimal cutting temperature medium (Tissue Tek), cryosectioned, and immunostained with anti-8-hydroxyguanosine (HGN), anti-nitro-tyrosine (N-Tyr), anti-sequestosome (p62), or anti-glial fibrillary acid protein (GFAP). ONL indicates the outer nuclear layer, INL the Inner nuclear layer. Scale bar represents 20 μm.

an antibody directed against activated caspase 3 (Fig. 3A). Contrary to what was expected, we did not observe a massive increase in active caspase 3 immunostaining, suggesting that this apoptotic pathway was not involved in cell death. This result drove our attention to the activation of caspase-independent pathways. We investigated first the activation of apoptosis inducing factor (AIF) (Fig. 3A). This pathway is activated by the release of AIF from the mitochondria to the nucleus, where it triggers chromatin condensation [16]. Immunohistochemistry analysis of LED-exposed retinas showed an increase of AIF staining in ONL and also in INL (Fig. 3A and Supplementary Fig. 8). However, although the nuclear layers of the retina were more stained than the control, it was not clear, due to the small amount of cytoplasm in photoreceptors, if the staining was really nuclear. To solve this point we counterstained our slides with an antibody against lamin B, a protein of the nuclear envelop, and we analyzed the section by confocal microscopy. As seen in Fig. 3B, upper panel, in light-exposed retinas AIF is located inside the nuclei where it forms small aggregates, suggesting the activation of this pathway.

We have previously shown that in light-induced retinal degeneration (LIRD) using white fluorescent bulbs, caspases were not activated [17]. Instead, a caspase-independent cell death pathway, the LEI/L-DNase II, was involved in photoreceptor degeneration [18]. The activation of this pathway involves cleavage, by specific proteases, of the cytoplasmic leukocyte elastase inhibitor (LEI), and its transformation into L-DNase II, a nuclear protein [19]. The nuclear translocation of this molecule was investigated as seen in Fig. 3A (and Supplementary Fig. 8). The same as for AIF, the staining of the nuclear layers of the retina was increased but the nuclear translocation was not clear. As for AIF we examined the sections after lamin B staining. Here again (Fig. 3B, lower panel) after white LED exposure L-DNase II was nuclearized but it was kept at the periphery of the condensed chromatin of the photoreceptor.

The high number of cells labeled by the TUNEL assay and the mild activation of caspase-dependent and caspase-independent effectors of cell death led us to investigate other mechanism that could be involved in photoreceptor demise, particularly those forms of cell death that could give TUNEL-positive labeling. We analyzed then the activation of programmed necrosis. This form of cell death is promoted and controlled by RIP kinases (receptor-interacting protein), a family of proteins that has been demonstrated to control and to promote necrosis [20]. We showed that RIP 1 and RIP 3 were increased under continuous light exposure conditions (Fig. 3A), suggesting an activation of necrosis. To verify this we analyzed the degradation pattern of poly-ADP-ribose polymerase 1 (Fig. 3C). During apoptosis, cleavage of PARP-1 by caspases 3 and 7 produced two fragments of 89 and 24 kDa [21]. During necrosis, however, a fragment of 62 kDa is produced [22,23]. A fragment of 44 kDa has also been described as the product of PARP-1 cleavage by calpain or cathepsin D [24]. In our experiments, after exposure to white LEDs (18 h, 125 J/cm^2), the 62 kDa fragment was clearly seen, as well as the fragment of 44 kDa. Moreover, a clear increase of the PARP-1 expression was seen in light-exposed retinas. This was concomitant with an increase of auto-ADP ribosylated PARP-1 (Fig. 3C, 250 kDa band). Taken together these data were in accord with the activation of necrosis.

In order to further document the activation of necrosis, histological and transmission electron microscopy (TEM) studies were performed to validate these findings and to explore morphological abnormalities of photoreceptors. Histological examination of semithin retinal sections showed that retina exposed to white LEDs for 18 h (125 J/cm^2) developed prominent interstitial spaces between photoreceptor nuclei and across the ONL (Supplementary Fig. 4). TEM showed a different alteration of photoreceptors according to the explored area (Fig. 4). At the POS (photoreceptor outer segment) level a complete disorganization of the ordered structure was seen after LED exposure. At the nuclei level several alterations were recorded. The dilation of the interphotoreceptor space was increased (white arrowhead), typical condensed nuclei, reminding apoptotic nuclei were seen (black arrow), as well as dilated nuclei reminding necrotic cells (white arrows). Alterations were also found at the PIS (photoreceptor inner segments): edema of the PIS, alteration of mitochondria (arrowhead), and edema of the endoplasmic reticulum (arrow). These are typical characteristics of necrotic cells.

Involvement of blue radiation in LED-induced damages

As seen in Supplementary Fig. 1, upper panel, the white LEDs used for the described experiments have an important emission in the blue region of the spectrum. In order to evaluate the effect of this blue light we conducted a new set of experiments where rats were exposed to blue LEDs. Four commercially available LEDs were used: the blue LED and the blue-green LED from Nichia Corporation (that we will call hereafter Nichia blue and Nichia blue-green, respectively), and the blue LED and the royal blue LED from Cree Industries (called hereafter Cree blue and Cree royal blue). The four LEDs were mounted in groups of four in the device described in Supplementary Fig. 2, designed and built for the intended experiments.

For blue LEDs almost the same parameters as for white LEDs were evaluated; however, the lesions found were more important so that we limited the exposure to 24 h. Fig. 5 shows representative results

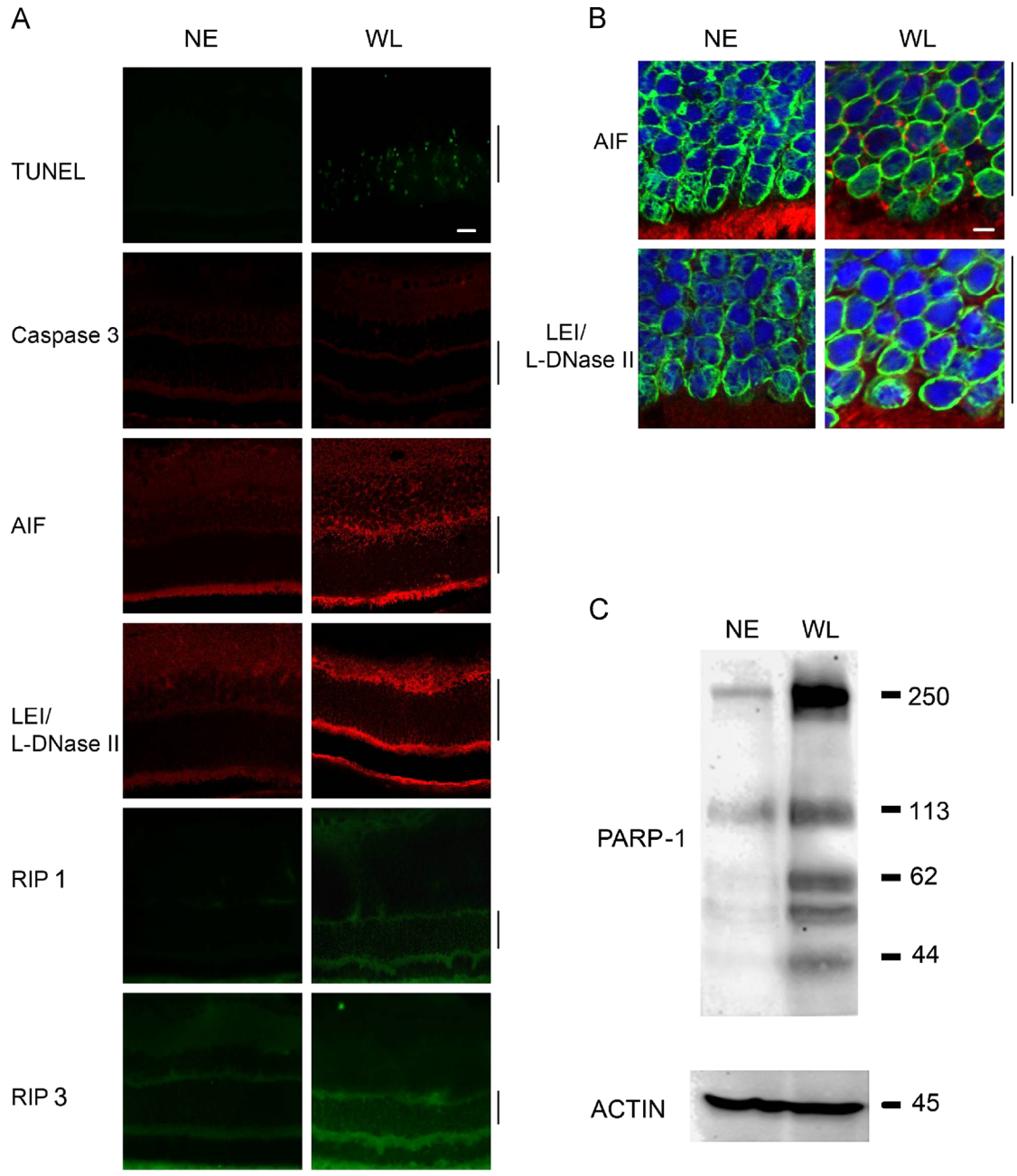

Fig. 3. The mechanisms of cell death in retina after white LED exposure. Male Wistar rats aged 7 weeks ($n=4$) were exposed to Xanlite XXX Evolution 5 W for 18 h. NE, Nonexposed rats; WL, rats exposed to white LEDs, 125 J/cm^2. At the end of the exposure period the eyes were analyzed regarding different effectors of cell death. (A) Eyes were stained with the TUNEL assay (TUNEL) or immunostained with anti-active-caspase 3 (caspase 3), anti-apoptosis inducing factor (AIF), anti-LEI derived DNase II (LEI/L-DNase II), anti-receptor-interacting protein (RIP 1) or anti-receptor-interacting protein kinase (RIP 3). Black vertical bars represent ONL. Scale bar represents 20 μm. (B) The outer nuclear layer was further analyzed by triple staining by confocal microscopy: (upper panel) anti-lamin B in green, anti-AIF in red, and DAPI in blue. In the lower panel the red fluorescence corresponds to anti-LEI/L-DNase II. Black vertical bars represent ONL. Scale bar represents 0.5 μm. (C) After light exposure the eyes were enucleated, and the retina was dissected, extracted with Laemmli sample buffer, loaded on the top of a 10% SDS-PAGE, transferred onto a nitrocellulose membrane, and probed for PARP-1. A control of charge has been made using an anti-actin on the same membrane after striping (actin).

of oxidative stress induction obtained after 18 h of exposure to the different LEDs. The increase of HGN labeling was comparable to the one obtained after white LED exposure, although the doses of exposure were quite different. However, Cree royal blue LEDs seemed to increase this marker of oxidative stress, mostly in the INL. Concerning N-Tyr, only the Cree royal blue LEDs produced the same degree of modification of the proteins at the RIS and ROS level as the white LEDs. As immunofluorescence is not a quantitative assay we investigated the difference in N-Tyr levels by Western blot (Fig. 5B). As seen in Fig. 5, blue diodes (but not Nichia blue-green) increased the nitric oxidation of tyrosines. The Cree royal blue presented the higher amount of nitrosylated proteins. Concerning the stress response, as with white LED, we also found an increase of p62. In order to compare the different diodes between them we evaluated p62 by Western blot after 18 h of exposure (Fig. 6A). We saw a global increase of p62 but, as it can be seen in Fig. 6A, the rate of cleavage of p62 is increased in Cree LEDs (CRB and CB). This cleavage is thought to disrupt the protective processes of autophagy and NFkB activation [25]. We investigated then the activation of both NFkB and PKC zeta (Fig. 6B and C, and Supplementary Fig. 9). PKC zeta is an upstream activator of NFkB that we have already seen activated in LIRD [59]. The activation of PKC zeta, as materialized by its phosphorylated

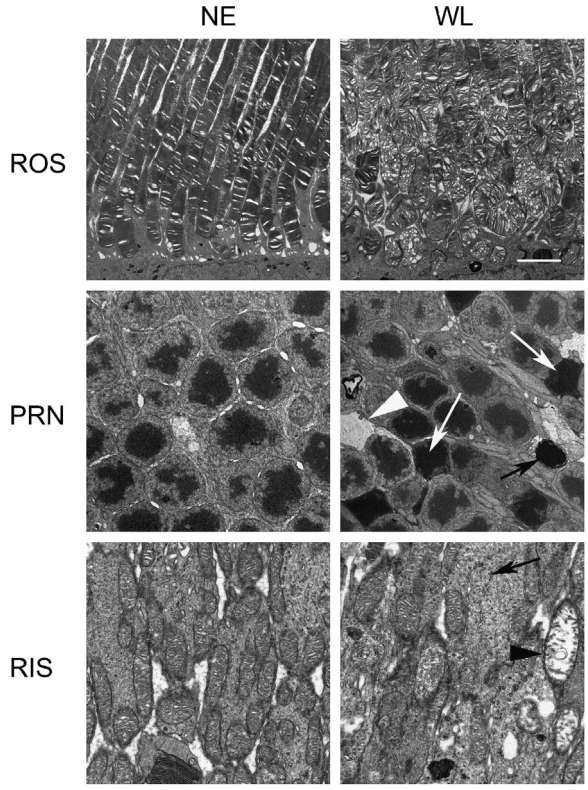

Fig. 4. Structural modifications of the retina examined by transmittance electron microscopy (TEM). Male Wistar rats aged 7 weeks ($n=4$) were exposed to Xanlite XXX Evolution 5 W for 18 h. At the end of the exposure period the eyes were analyzed by TEM. NE, nonexposed animals; WL, exposed animals to white LED (125 J/cm^2). ROS, rod outer segments; PRN, photoreceptor nuclear layer also called ONL. RIS: rod inner segment layer. In PRN panels white arrowhead shows dilated interphotoreceptors spaces, black arrow an apoptotic cell, and white arrows necrotic nuclei. RIS panels: arrowhead indicates dilated mitochondria; black arrow dilated endoplasmic reticulum. Scale bar represents 0.5 μm.

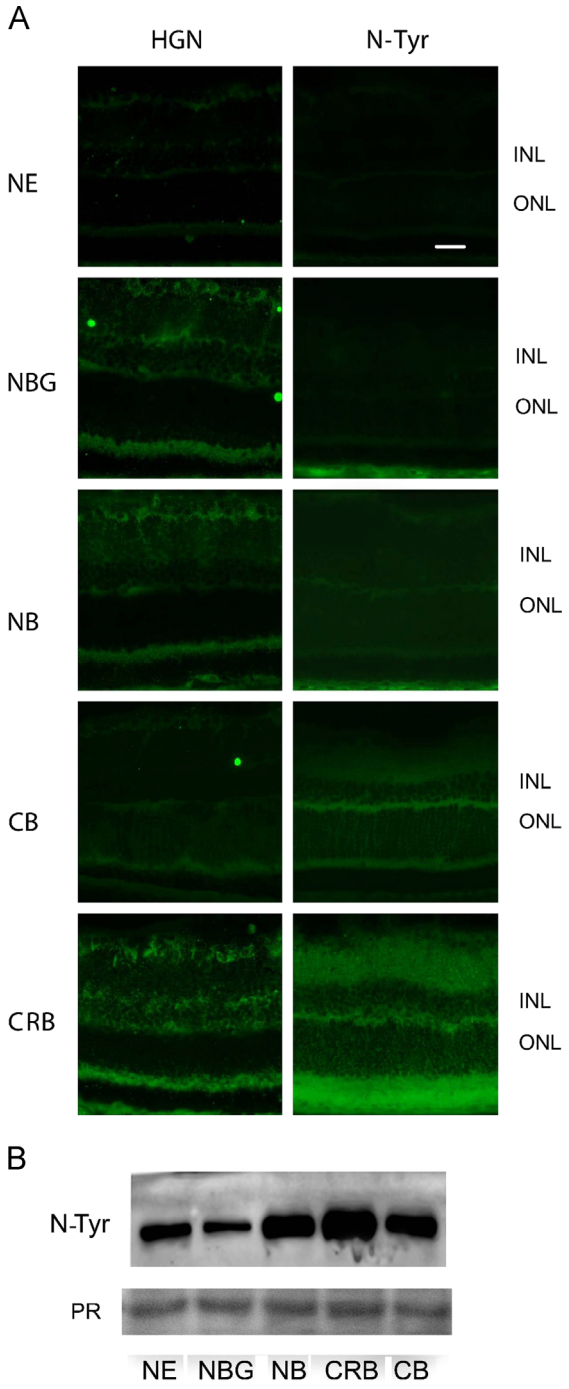

Fig. 5. Oxidative stress response after blue LED exposure. Male Wistar rats aged 7 weeks ($n=4$) were exposed to Nichia blue-green LEDs (NBG), Nichia blue LEDs (NB), Cree blue LEDs (CB), or Cree royal blue LEDs (CRB) for 18 h. NE: nonexposed animals. (A) The immunoreactivity of the retinas using an anti-8-hydroxyguanosine (HGN) or an anti-nitro-tyrosine (N-Tyr) antibodies. Scale bar represents 20 μm. (B) After light exposure the eyes were enucleated, and the retina was dissected, extracted with M-PER (Pierce) buffer, loaded on the top of a 12% SDS-PAGE, transferred onto a nitrocellulose membrane, and probed for nitro-tyrosine. Ponceau Red (PR) labeling was used as a charge control.

form, seemed activated in all but Nichia blue-green LEDs. This is also the case for phospho-NFkB, suggesting that the stress induced by pure blue LEDs was different from the stress induced by an almost green device. It is interesting to note that the PKC zeta pattern was completely different when rats were exposed to Nichia blue-green radiation. This was the only situation in which a cleavage of the enzyme was seen (Fig. 6B).

Taken together these results indicated that the blue-rich light induced a more profound cellular stress, mainly affecting photoreceptors. This cellular stress induced a proportional cellular response.

We next investigated the toxicity of the blue LEDs by examining cell death, as before. TUNEL labeling indicated the presence of dying photoreceptors in all situations (Fig. 7). Interestingly, when we looked for caspase 3 activation, cleaved caspase 3 labeling was only found in INL after blue LED exposure. This was different from white LEDs, where no activation of caspase 3 was found (Fig. 3). Moreover, it was surprising to see such an important activation of caspase 3 without a single TUNEL-positive cell in the INL layer.

Following the same scheme as that for white LEDs, we evaluated caspase-independent pathways. This was done after 18 h of LED exposure. Results are seen in Fig. 8. AIF seemed activated only in Nichia blue-green LEDs, as indicated by the presence of truncated AIF (Fig. 8A, upper panel, arrowhead). L-DNase II is also activated (Fig. 8A, middle panel) but in a different way, as seen in Fig. 8A. Lower panel shows the quantification of the ratio L-DNase II/LEI. L-DNase II is activated in blue-rich LEDs (CRB, CB, and NB), and this activation is the most important in Cree royal blue LEDs.

In order to evaluate the presence of necrosis we studied RIP 1 and RIP 3 after 18 h of exposure to LEDs. RIP 1 was cleaved when using Cree devices, indicating the presence of necrosis, while RIP 3 was clearly cleaved when rats were exposed to Nichia blue-green light. As this fragment is usually produced by caspase 8 we looked for the activation of this enzyme. The lower panel of Fig. 8B shows a

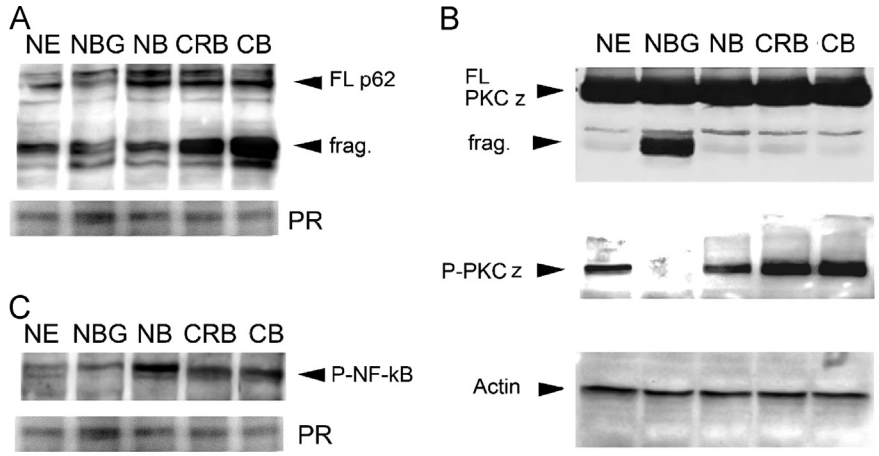

Fig. 6. Western blot analysis of retinas from animals exposed to blue LEDs. Male Wistar rats aged 7 weeks ($n=4$) were exposed to Nichia blue-green LEDs (NBG), Nichia blue LEDs (NB), Cree blue LEDs (CB), or Cree royal blue LEDs (CRB) for 18 h. NE: nonexposed animals. After light exposure the eyes were enucleated, and the retina was dissected, extracted with M-PER (Pierce) buffer, loaded on the top of a 12% SDS-PAGE, transferred onto a nitrocellulose membrane, and probed with different antibodies. (A) anti-p62: FL p62 indicates the full-length molecule; fragment indicates the cleaved molecule. PR indicates Ponceau Red staining. (B) anti-PKC zeta: The upper panel was made using an anti-PKC zeta. Full-length and cleaved species are indicated. Middle panel was performed using an anti-PPKC zeta (phosphor-Thr 410). The lower panel is a charge control using actin. (C) The Western blot membrane was probed with anti-phospho-NFkB, ser 311. These are representative results of three independent experiments. PR indicates Ponceau Red staining.

representative experiment of this study in which the upper band represents the procaspase 8, while the lower band (arrowhead) represents the active caspase 8. Taken together these results indicate the activation by blue light of caspase-independent pathways, but mostly the activation of necrosis.

The activation of this form of cell death is rare in light-induced retinal degeneration; thus, we tried to prove that necrosis was really taking place in the retinas of exposed rats. To do this we used the property of propidium iodide (PI) to label the nuclei of a cell that has lost the integrity of its membrane. To label photoreceptors we injected intravitreally a PI solution after LED exposure, some minutes before sacrifice. The eyes were then enucleated and immediately fixed, mounted, cryosectioned, and observed with a fluorescence microscope without any other type of treatment or staining. Fig. 8C shows a representative result of these experiments. Exposed retinas show a very high number of labeled cells situated in the inner part of the ONL. The combination of this technique with a TUNEL staining (Fig. 8C lower panel) clearly shows the presence of TUNEL-positive, PI-negative cells. These were apoptotic cells, and PI-positive cells that were necrotic cells whether they were or not TUNEL positive.

These data confirmed the degeneration induced by LED light on the retina, indicating a structural loss of photoreceptors and the activation of two cell death pathways: apoptosis and necrosis.

The Western blot analysis of white LED-exposed retinas (18 h, 125 J/cm^2) shows patterns of the above-studied molecular markers corresponding to Nichia blue-green and Nichia blue LEDs, indicating that these forms of cell demise are also activated by the white LEDs (Fig. 8D).

Discussion

In this paper we analyzed the effects of the so-called “white LEDs” and blue-enriched LEDs on the retina. We show an important damage of the photoreceptors layer after 18 h of exposure. More importantly, the analysis, at the molecular level, of the effectors of cell death shows an activation of necrotic cell death, a rare event in this type of degeneration.

The current regulation [26] establishes that light is toxic to the eye when there is a bleaching of the retina as seen by fundoscopy. In our macroscopic analysis the eyes of rats exposed to LED light show no bleaching, but an important chemosis. This indicates an edema of the ocular tissues, a sign of eye irritation, probably due to exudation from abnormally permeable capillaries and a conjunctival vasodilation. It is surprising and unexpected that the LED-exposed eye suffers from an important edema without detectable damage to the retina by fundus examination. This also suggests that there are probably invisible photochemical lesions. Actually, our study shows the presence of important oxidative damage, involving proteins and nucleic acids, as well as an important amount of cell death. In 2001, the Dawson study showed that blue LEDs (460 nm) and argon laser (458 nm) lead to the same retinal lesions with corneal irradiance of 10 J/cm^2 [27]. These results were confirmed by Ueda's team that showed retinal damages at the macula with blue LEDs (465 nm) [28]. In every case the used devices were almost experimental, while in the present study we used commercially available sources. Moreover, irradiance fluxes were about 1/20 those used in the Dawson experiments (our LEDs induce a corneal irradiance of about 0.0026 W/cm^2). Recently, a study of Mukai et al. showed that retinas of monkeys exposed to LED light for 8 h present intracellular vacuoles in the outer segments of photoreceptors, a feature also seen in our study. This study also show that these structural lesions are accompanied by functional alterations revealed by an ERG study showing a decreased response of rods and cones [29], but the mechanisms of the toxicity were not analyzed.

In this study we analyzed the molecular mechanisms of retinal damage. We used the usual model of albino rats. Although the pertinence of this model and the translation of the results to human beings are matters of discussion, it is useful to gain an idea of the kind of lesions found with these new devices as compared with others already investigated in our laboratory [17,18].

Phototoxicity depends mainly on intensity of the radiation, its exposure time and its spectrum, as showed by Knels's team who used two types of LEDs (411 nm blue and 470 nm green) on a line of R28 retinal cells [30]. This *in vitro* study revealed activation of the antioxidant system involving glutathione in cells illuminated regardless of exposition, spectrum, and power of LEDs. In our model we also found signs of oxidative stress, as revealed by the increased labeling in HGN and N-Tyr, reflecting the oxidation of DNA/RNA and proteins, respectively. This oxidative stress seems to be more important with blue light. In our hands the Cree royal blue LEDs produced a higher degree of protein oxidation (as seen by N-Tyr Western blot) than the other blue LEDs, although the doses of exposure were quite similar (e.g., 42.3 J/cm^2 for Nichia blue and 34.2 for Cree royal blue).

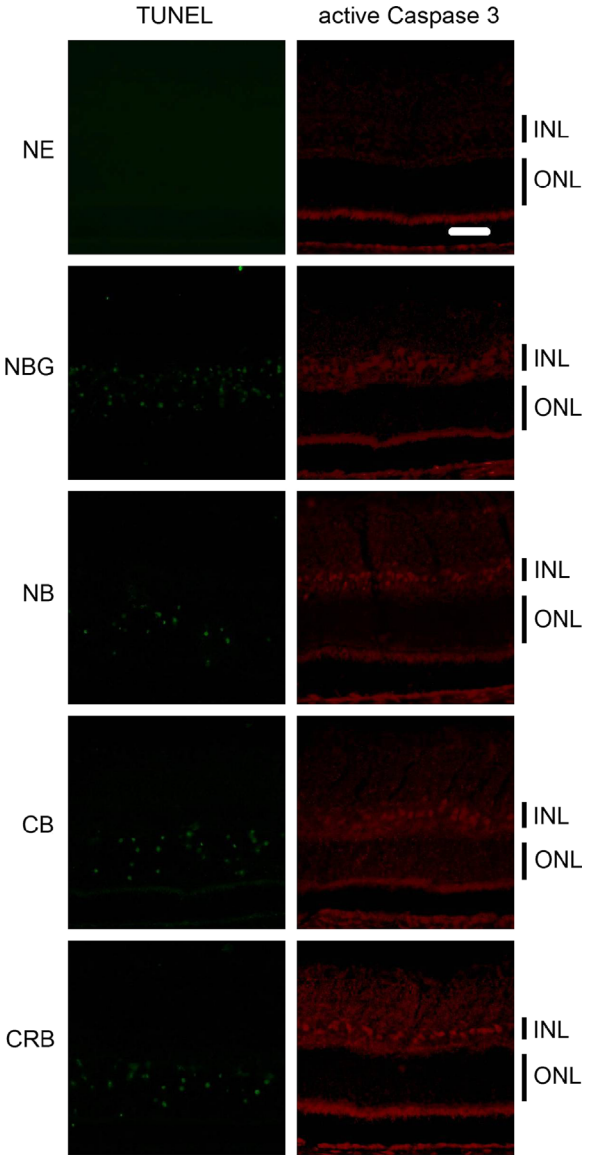

Fig. 7. The induction of classical apoptosis in blue LED-exposed retinas. Male Wistar rats aged 7 weeks ($n=4$) were exposed to Nichia blue-green LEDs (NBG), Nichia blue LEDs (NB), Cree blue LEDs (CB), or Cree royal blue LEDs (CRB) for 18. At the end of the exposure period the eyes were analyzed using the TUNEL assay (green) and anti-active-caspase 3 (red). INL, Inner nuclear layer; ONL, outer nuclear layer. Scale bar represents 20 μm.

The oxidative stress induces a retinal response unrevealed by a reaction of Müller cells though the increased expression of GFAP, a well-known sign of retinal stress (Fig. 2 and Supplementary Fig. 5). The increase of GFAP expression is thought to help in maintaining the integrity of the macroglial network under stress conditions [31]. The stress generating this reaction could be the oxidative stress *per se*, but also a mechanical stress generated by the intercellular edema that we described (Supplementary Fig. 4).

Another stress response concerns the p62 protein (sequestosome 1). This is a multifunctional ubiquitin-binding scaffolding protein involved in autophagy and also in oxidative stress [32]. It is thought to be a proteotoxic stress response protein [33]. Eighteen hours of white LED exposure induced a nuclear immunostaining of p62 especially in the INL but also in the ONL and GCL. This nuclear translocation of p62 was described as being a disruption of the nuclear–cytoplasmic shuttling of p62 [34]. In order to investigate the role of the blue part of the light spectrum in p62 expression, we used Western blotting analysis of illuminated retina after 18 h of LED exposure with green and blue LEDs. We observed an increase of the entire form of p62 with blue LEDs (449, 467, and 473 nm), contrary to green LEDs (507 nm) and nonexposed retina. Furthermore, we observed cleavage of p62 revealed by two new bands with apparent molecular weights of 46 and 37 kDa. These N-terminal fragments of p62 correspond to the cleavage by caspase 8 which seems to occur when there is autophagy impairment, a state that promotes apoptosis [35] or autophagic cell death [36]. The immunoreactive bands corresponding to the cleaved fragments are more intense in the retinas illuminated with blue LEDs (449, 467, and 473 nm) with respect to green LEDs (507 nm), suggesting a stronger alteration of basal autophagy and a stronger promotion of cell death.

The stress generated by LED exposure induces the cell stress responses discussed above, concomitantly with survival-promoting signals. Among the possible responses of the retinal cells we investigated the PKC zeta-NFkB axis, because it was shown to be largely involved in other responses to retinal damage, as in diabetic retinopathy [37] and even in light damage (unpublished results). Following stress, activated PKC zeta phosphorylates IKK (Ikappa kinase B), which phosphorylates IKB leading to the release of NFkB and its nuclear translocation [38]. NFkB promotes the transcription of antiapoptotic genes such as Bcl-2, IAP, and TRAF1/2 (TNF receptor-associated factors) [39]. Eighteen hours of LED exposure induced a nuclear immunostaining of phospho-NFkB in the INL and GCL absent in nonexposed retina. The nuclear staining seems to be more intense in INL after the illumination with blue LEDs (NB, CRB, and CB). This result was confirmed by Western blotting analysis using the same antibody that recognizes the phosphorylated serine 311 form of NFkB, which is a specific substrate of the PKC zeta pathway [40]. PKC zeta typically has a biphasic response, which is protective when activated and promoting cell death when cleaved. Cleavage of PKC zeta corresponds to a constitutive activated form of PKC zeta mediated by the caspase pathway [41,42]. The phosphorylation of threonine 410 of PKC zeta corresponds to the activated enzyme which in turn induces a phosphorylation cascade of other proteins to transducer stress signals. Western blot using phospho-PKC zeta antibody revealed an increase of the phosphorylated PKC zeta (band of 72 kDa) in the retina exposed to blue LEDs (449, 467, and 473 nm) compared to nonexposed retina, suggesting the involvement of PKC zeta pathway in the stress response after exposure. To note, the exposure to the Nichia blue-green LEDs produces a different reaction with a cleavage of the enzyme not seen under the other conditions. This fact, together with the presence of many TUNEL-positive cells, suggests that the protective signals are overwhelmed, triggering cell death.

Among the different forms of cell death, apoptosis is the best known and it has been largely involved in retinal degeneration [9,10]. Although our group and others have shown the lack of caspase activation in light-induced retinal degeneration [17,43], the presence of the PKC zeta fragment suggested caspase activation. We investigate this issue by using an anti-active-caspase 3 antibody. Surprisingly, no label was found in the ONL, the layer where the TUNEL-positive cells accumulate, but in the INL, where not a single TUNEL-positive cell was seen in all the experiments we have performed, not even when using very long times of exposure.

We have then cells that are dying, owing to their TUNEL positivity, but that are active-caspase 3 negative. This kind of situation can be found in caspase-independent apoptosis, in necroptosis, or in necrosis. In order to gain more insight into this issue, we investigated the state of PARP-1.

PARP-1 is known for its role in DNA repair [44]. During apoptosis, cleavage of PARP-1 by caspases 3 and 7 has become a useful hallmark of this type of cell death [21]. The caspase cleavage of PARP-1 generates a catalytic fragment of 89 and a 24 kDa fragment corresponding to the DNA-binding domain. Interestingly, PARP-1 is also cleaved during necrosis but in this situation it generates a 62 kDa

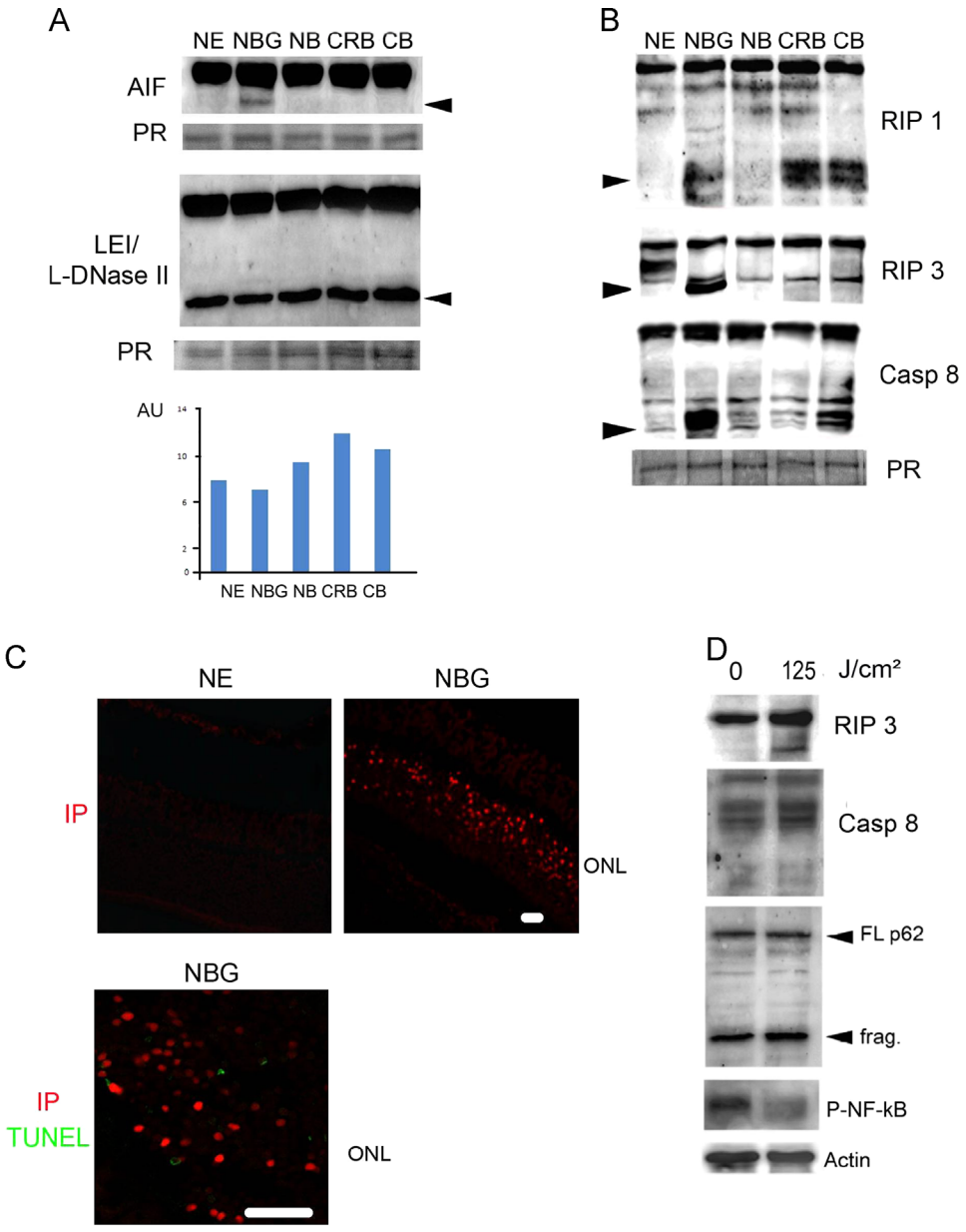

Fig. 8. The mechanisms of cell death in retina after blue LED exposure. Male Wistar rats aged 7 weeks ($n=4$) were exposed to Nichia blue-green LEDs (NBG), Nichia blue LEDs (NB), Cree blue LEDs (CB), or Cree royal blue LEDs (CRB) for 18 h. NE: nonexposed animals. At the end of the exposure period the eyes were analyzed regarding different effectors of cell death. (A) After light exposure the eyes were enucleated, and the retina was dissected, extracted with M-PER buffer, loaded on the top of a 12% SDS-PAGE, transferred onto a nitrocellulose membrane, and probed for apoptosis inducing factor (AIF) (upper panel), LEI derived DNase II (LEI/L-DNase II) (middle panel). In both panels the arrowhead indicates the cleaved and therefore activated molecule. The lower panel indicates the quantification of the active L-DNase II as compared to LEI, its precursor. Ponceau red staining was used as the loading control. (B) Same experiment as that in panel A using anti-receptor-interacting protein 1 and 3 (RIP 1 and RIP 3, respectively) (upper and middle panels) or anti-caspase 8 (lower panel). The arrowheads indicate the cleaved forms of the different molecular species. PR indicates Ponceau Red staining. (C) After an intravitreal injection of propidium iodide (PI) the eyes were fixed, cryosectioned, and examined under a fluorescence microscope. Bright nuclei belong to necrotic cells. The lower panel shows the same experiment in which a TUNEL assay has been performed after cryosection. Scale bar represents 20 μm. (D) After exposure to white LED for 18 h the eyes were enucleated, and the retina dissected, extracted with M-PER buffer, loaded on the top of a 12% SDS-PAGE, transferred onto a nitrocellulose membrane, and probed with RIP 3, caspase 8, p62, and phospho-NFkB. Actin was used as a charge control.

fragment [22]. After 18 h of exposure to white LEDs, Western blot analysis showed different patterns between exposed and unexposed rats. We observed a band with very high molecular weight (250 kDa) corresponding to the automodified PARP-1. Automodification of PARP-1 by poly (ADP-ribose) is involved in its interaction with damaged DNA and it is thought to upregulate the NFkB/DNA complex [45]. The expression of PARP-1 (113 kDa) is also increased. Moreover, we found the 62 kDa fragment, suggesting the existence of a necrotic cell death after LED exposure. Additionally, a band of approximately 44/42 kDa is observed that could be the fragment generated after cleavage of PARP-1 by calpain or cathepsin D, as described by Chaitanya et al. [24]. These elements support a cell death by necrosis.

To validate the existence of necrosis and evaluate the weight of blue light in its activation we analyzed the expression of RIP 1 and RIP 3 kinases by Western blot (Fig. 8). Both RIP 1 and RIP 3 were slightly increased in all exposed retinas. The 42/40 kDa doublets observed were described as the C-terminal death domain-containing portion of RIP 1 kinase [46]. The cleavage of RIP 1 kinase abolishes its anti-apoptotic effect by impairing its capacity to induce NFkB [47]. The study of RIP 3 kinase also revealed a cleaved form of 39 kDa in retina

exposed to green LEDs (NBG). This is a product of caspase 8 that is also activated (Fig. 8). It is important to note that cleavage of RIP 3 by caspase 8 inactivates this protein due to the loss of its kinase domain and its ability to form the necrosome, a key stage of necrosis [48]. Due to their interaction with death receptors and their ability to form the necrosome, RIP 1 and RIP 3 kinases control the switch between apoptotic and necrotic cell death [49]. Taken together these results indicate that the greener LEDs (NBG) tend to induce apoptotic cell death, while the blue radiation tends to induce necrotic cell death (CRB and CB). We further explored this point by analyzing caspase-independent effectors of cell death such as AIF [16] and LEI/L-DNase II [50]. Both effectors were modestly activated in ONL during early exposure, while L-DNase II seems massively activated at later times (24 h). This is not surprising since this system is usually activated by metabolic stress [51]. It is also interesting to note that AIF and L-DNase II activation can be mediated by the activation of calpain 1, the first directly, by cleavage and release from the mitochondrial inner membrane [52,53], the second indirectly, by permeabilizing lysosomes and releasing cathepsin D [54]. Moreover, although theses effectors have originally been described as mediating apoptosis, AIF has been shown to mediate necroptosis [55] and LEI/L-DNase II, due to its activation by lysosomal enzymes, could be also an effector of necrosis [56].

We further investigated the presence of necrosis by staining cells with PI. This DNA binding dye is very useful in characterizing cell death. It is used routinely in flow cytometry because of its capacity to enter the cell and label DNA when the plasma membrane is damaged. We performed then an intravitreal injection of this dye some minutes before the sacrifice of the animal. Interestingly, a very high number of photoreceptors were labeled, much more than photoreceptors that are TUNEL positive, indicating that permeabilization of the plasma membrane precedes degradation of DNA.

The existence of this necrosis easily explains the presence of retinal edema seen in the histological sections, an edema that is not subretinal but interstitial. This could also explain the presence of an early inflammatory reaction, probably due to the release of DAMPS (damage-associated molecular-pattern molecules) [57] that may also be responsible for the chemosis seen in the exposed rats.

Using a comparable set of experiments Shang's team recently show that white LEDs lead to photoreceptors death [58], with an important oxidative stress, as we confirmed in this paper; however, according to our data, apoptosis is not the major pathway involved in photoreceptor demise. Actually, the experimental design of Shang et al. has several differences from ours but two differences are very important: first they use dark-adapted animals, a procedure that increases retinal sensitivity to light. Second, they evaluate the retinal damage after a recovery period, allowing the tissue to eventually repair. In our experimental setup we analyzed the eyes just after exposure in order to investigate the mechanism of cell death activated during degeneration.

Taken together these data indicate that the blue component of the LED is the major cause of retinal damage, as has been previously predicted [12]. In addition, current regulation establishes that for an exposure greater than 10,000 s, ELV, expressed in term of blue light radiance, is about 100 $W/m^2/sr$ [14], largely over the radiances used in this study (Table 1), suggesting that these regulations should be reevaluated by transposing our results to the human eye.

Moreover, the reduced size of LEDs allows the production of composite sources of very high luminance. This introduces a cautionary note on their use in domestic lighting that needs to be extremely controlled to remain safe for vision.

Acknowledgments

This work was supported by INSERM, ENVA, CSTB, and by an ADEME financial support (RETINALED project). I.J. has a fellowship from ADEME. The authors are indebted to Dr. Patricia Lassiaz for helpful discussions on PKC zeta and to Mrs. Brigitte Goldenberg and Mr. Christophe Klein for technical assistance.

Appendix A. Supporting information

Supplementary data associated with this article can be found in the online version at http://dx.doi.org/10.1016/j.freeradbiomed.2015.03.034.

References

[1] Cheung, L. K.; Eaton, A. Age-related macular degeneration. *Pharmacotherapy* **33:**838–855; 2013.
[2] Paskowitz, D. M.; LaVail, M. M.; Duncan, J. L. Light and inherited retinal degeneration. *Br. J. Ophthalmol.* **90:**1060–1066; 2006.
[3] Blasiak, J.; Salminen, A.; Kaarniranta, K. Potential of epigenetic mechanisms in AMD pathology. *Front. Biosci. (Schol. Ed.)* **5:**412–425; 2013.
[4] Sui, G. Y.; Liu, G. C.; Liu, G. Y.; Gao, Y. Y.; Deng, Y.; Wang, W. Y.; Tong, S. H.; Wang, L. Is sunlight exposure a risk factor for age-related macular degeneration? A systematic review and meta-analysis *Br. J. Ophthalmol.* **97:**389–394; 2013.
[5] Hirai, F. E.; Moss, S. E.; Knudtson, M. D.; Klein, B. E.; Klein, R. Retinopathy and survival in a population without diabetes: the Beaver Dam Eye Study. *Am. J. Epidemiol.* **166:**724–730; 2007.
[6] Klein, R.; Klein, B. E.; Knudtson, M. D.; Meuer, S. M.; Swift, M.; Gangnon, R. E. Fifteen-year cumulative incidence of age-related macular degeneration: the Beaver Dam Eye Study. *Ophthalmology* **114:**253–262; 2007.
[7] Noell, W. K.; Walker, V. S.; Kang, B. S.; Berman, S. Retinal damage by light in rats. *Invest. Ophthalmol* **5:**450–473; 1966.
[8] Organisciak, D. T.; Darrow, R. A.; Barsalou, L.; Darrow, R. M.; Lininger, L. A. Light-induced damage in the retina: differential effects of dimethylthiourea on photoreceptor survival, apoptosis and DNA oxidation. *Photochem. Photobiol.* **70:**261–268; 1999.
[9] Reme, C. E.; Grimm, C.; Hafezi, F.; Wenzel, A.; Williams, T. P. Apoptosis in the retina: the silent death of vision. *News Physiol. Sci.* **15:**120–124; 2000.
[10] Reme, C. E.; Grimm, C.; Hafezi, F.; Marti, A.; Wenzel, A. Apoptotic cell death in retinal degenerations. *Prog. Retin. Eye Res.* **17:**443–464; 1998.
[11] Behar-Cohen, F.; Martinsons, C.; Vienot, F.; Zissis, G.; Barlier-Salsi, A.; Cesarini, J. P.; Enouf, O.; Garcia, M.; Picaud, S.; Attia, D. Light-emitting diodes (LED) for domestic lighting: any risks for the eye? *Prog. Retin. Eye Res.* **30:**239–257; 2011.
[12] van Norren, D.; Gorgels, T. G. The action spectrum of photochemical damage to the retina: a review of monochromatic threshold data. *Photochem. Photobiol.* **87:**747–753; 2011.
[13] Torriglia, A.; Chaudun, E.; Chany-Fournier, F.; Jeanny, J. C.; Courtois, Y.; Counis, M. F. Involvement of DNase II in nuclear degeneration during lens cell differentiation. *J. Biol. Chem.* **270:**28579–28585; 1995.
[14] Matthes, R.; Feychting, M.; Ahlbom, A.; Breitbart, E.; Croft, R.; de Gruijl, F.; Green, A.; Hietanen, M.; Jokela, K.; Lin, J. Icnirp guidelines on limits of exposure to incoherent visible and infrared radiation. *Health Phys.* **105:**74–91; 2013.
[15] Huxlin, K. R.; Dreher, Z.; Schulz, M.; Dreher, B. Glial reactivity in the retina of adult rats. *Glia* **15:**105–118; 1995.
[16] Susin, S. A.; Lorenzo, H. K.; Zamzami, N.; Marzo, I.; Snow, B. E.; Brothers, G. M.; Mangion, J.; Jacotot, E.; Costantini, P.; Loeffler, M.; Larochette, N.; Goodlett, D. R.; Aebersold, R.; Siderovski, D. P.; Penninger, J. M.; Kroemer, G. Molecular characterization of mitochondrial apoptosis-inducing factor. *Nature* **397:**441–446; 1999.
[17] Chahory, S.; Keller, N.; Martin, E.; Omri, B.; Crisanti, P.; Torriglia, A. Light induced retinal degeneration activates a caspase-independent pathway involving cathepsin D. *Neurochem. Int.* **57:**278–287; 2010.
[18] Chahory, S.; Padron, L.; Courtois, Y.; Torriglia, A. The LEI/L-DNase II pathway is activated in light-induced retinal degeneration in rats. *Neurosci. Lett.* **367:**205–209; 2004.
[19] Padron-Barthe, L.; Lepretre, C.; Martin, E.; Counis, M. F.; Torriglia, A. Conformational modification of serpins transforms leukocyte elastase inhibitor into an endonuclease involved in apoptosis. *Mol. Cell. Biol.* **27:**4028–4036; 2007.
[20] Galluzzi, L.; Kepp, O.; Kroemer, G. RIP kinases initiate programmed necrosis. *J. Mol. Cell. Biol.* **1:**8–10; 2009.
[21] Kaufmann, S. H.; Desnoyers, S.; Ottaviano, Y.; Davidson, N. E.; Poirier, G. G. Specific proteolytic cleavage of poly(ADP-ribose) polymerase: an early marker of chemotherapy-induced apoptosis. *Cancer Res.* **53:**3976–3985; 1993.
[22] Gobeil, S.; Boucher, C. C.; Nadeau, D.; Poirier, G. G. Characterization of the necrotic cleavage of poly(ADP-ribose) polymerase (PARP-1): implication of lysosomal proteases. *Cell Death Differ.* **8:**588–594; 2001.
[23] Boucher, C.; Gobeil, S.; Samejima, K.; Earnshaw, W. C.; Poirier, G. G. Identification and analysis of caspase substrates: proteolytic cleavage of poly (ADP-ribose)polymerase and DNA fragmentation factor 45. *Methods Cell Biol.* **66:**289–306; 2001.

[24] Chaitanya, G. V.; Steven, A. J.; Babu, P. P. PARP-1 cleavage fragments: signatures of cell-death proteases in neurodegeneration. *Cell Commun. Signal* **8:**31; 2010.
[25] Shi, J.; Wong, J.; Piesik, P.; Fung, G.; Zhang, J.; Jagdeo, J.; Li, X.; Jan, E.; Luo, H. Cleavage of sequestosome 1/p62 by an enteroviral protease results in disrupted selective autophagy and impaired NFKB signaling. *Autophagy* **9:**1591–1603; 2013.
[26] Martinsons, C.; Zissis, G. Potential Health Issues of Solid-State Lighting, Report of the International Energy Agency, Energy Efficient End-Use Equipment (4E), SSL Annex,. ⟨http://ssl.iea-4e.org/task-1-quality-assurance/health-aspects-report⟩; 2014.
[27] Dawson, W.; Nakanishi-Ueda, T.; Armstrong, D.; Reitze, D.; Samuelson, D.; Hope, M.; Fukuda, S.; Matsuishi, M.; Ozawa, T.; Ueda, T.; Koide, R. Local fundus response to blue (LED and laser) and infrared (LED and laser) sources. *Exp. Eye Res.* **73:**137–147; 2001.
[28] Ueda, T.; Nakanishi-Ueda, T.; Yasuhara, H.; Koide, R.; Dawson, W. W. Eye damage control by reduced blue illumination. *Exp. Eye Res.* **89:**863–868; 2009.
[29] Mukai, R.; Akiyama, H.; Tajika, Y.; Shimoda, Y.; Yorifuji, H.; Kishi, S. Functional and morphologic consequences of light exposure in primate eyes. *Invest. Ophthalmol. Vis. Sci.* **53:**6035–6044; 2012.
[30] Knels, L.; Valtink, M.; Roehlecke, C.; Lupp, A.; de la Vega, J.; Mehner, M.; Funk, R. H. Blue light stress in retinal neuronal (R28) cells is dependent on wavelength range and irradiance. *Eur. J. Neurosci.* **34:**548–558; 2011.
[31] Lundkvist, A.; Reichenbach, A.; Betsholtz, C.; Carmeliet, P.; Wolburg, H.; Pekny, M. Under stress, the absence of intermediate filaments from Müller cells in the retina has structural and functional consequences. *J. Cell Sci.* **117:**3481–3488; 2004.
[32] Nezis, I. P.; Stenmark, H. p62 at the interface of autophagy, oxidative stress signaling, and cancer. *Antioxid. Redox Signal.* **17:**786–793; 2012.
[33] Geetha, T.; Wooten, M. W. Structure and functional properties of the ubiquitin binding protein p62. *FEBS Lett.* **512:**19–24; 2002.
[34] Pankiv, S.; Lamark, T.; Bruun, J. A.; Overvatn, A.; Bjorkoy, G.; Johansen, T. Nucleocytoplasmic shuttling of p62/SQSTM1 and its role in recruitment of nuclear polyubiquitinated proteins to promyelocytic leukemia bodies. *J. Biol. Chem.* **285:**5941–5953; 2010.
[35] Norman, J. M.; Cohen, G. M.; Bampton, E. T. The in vitro cleavage of the hAtg proteins by cell death proteases. *Autophagy* **6:**1042–1056; 2010.
[36] Giansanti, V.; Rodriguez, G. E.; Savoldelli, M.; Gioia, R.; Forlino, A.; Mazzini, G.; Pennati, M.; Zaffaroni, N.; Scovassi, A. I.; Torriglia, A. Characterization of stress response in human retinal epithelial cells. *J. Cell. Mol. Med.* **17:**103–115; 2013.
[37] Omri, S.; Behar-Cohen, F.; Rothschild, P. R.; Gelize, E.; Jonet, L.; Jeanny, J. C.; Omri, B.; Crisanti, P. PKCzeta mediates breakdown of outer blood-retinal barriers in diabetic retinopathy. *PLoS One* **8:**e81600; 2013.
[38] Hirai, T.; Chida, K. Protein kinase Czeta (PKCzeta): activation mechanisms and cellular functions. *J. Biochem.* **133:**1–7; 2003.
[39] Li, X.; Stark, G. R. NFkappaB-dependent signaling pathways. *Exp. Hematol.* **30:**285–296; 2002.
[40] Duran, A.; Diaz-Meco, M. T.; Moscat, J. Essential role of RelA Ser311 phosphorylation by zetaPKC in NF-kappaB transcriptional activation. *EMBO J.* **22:**3910–3918; 2003.
[41] Smith, L.; Chen, L.; Reyland, M. E.; DeVries, T. A.; Talanian, R. V.; Omura, S.; Smith, J. B. Activation of atypical protein kinase C zeta by caspase processing and degradation by the ubiquitin-proteasome system. *J. Biol. Chem.* **275:**40620–40627; 2000.
[42] Smith, L.; Smith, J. B. Lack of constitutive activity of the free kinase domain of protein kinase C zeta. Dependence on transphosphorylation of the activation loop. *J. Biol. Chem.* **277:**45866–45873; 2002.
[43] Donovan, M.; Carmody, R. J.; Cotter, T. G. Light-induced photoreceptor apoptosis in vivo requires neuronal nitric-oxide synthase and guanylate cyclase activity and is caspase-3-independent. *J. Biol. Chem.* **276:**23000–23008; 2001.
[44] Dantzer, F.; Schreiber, V.; Niedergang, C.; Trucco, C.; Flatter, E.; De La Rubia, G.; Oliver, J.; Rolli, V.; Menissier-de Murcia, J.; de Murcia, G. Involvement of poly (ADP-ribose) polymerase in base excision repair. *Biochimie* **81:**69–75; 1999.
[45] Nakajima, H.; Nagaso, H.; Kakui, N.; Ishikawa, M.; Hiranuma, T.; Hoshiko, S. Critical role of the automodification of poly(ADP-ribose) polymerase-1 in nuclear factor-kappaB-dependent gene expression in primary cultured mouse glial cells. *J. Biol. Chem.* **279:**42774–42786; 2004.
[46] Lin, Y.; Devin, A.; Rodriguez, Y.; Liu, Z. G. Cleavage of the death domain kinase RIP by caspase-8 prompts TNF-induced apoptosis. *Genes Dev.* **13:**2514–2526; 1999.
[47] Ting, A. T.; Pimentel-Muinos, F. X.; Seed, B. RIP mediates tumor necrosis factor receptor 1 activation of NF-kappaB but not Fas/APO-1-initiated apoptosis. *EMBO J.* **15:**6189–6196; 1996.
[48] Moriwaki, K.; Chan, F. K. RIP3: a molecular switch for necrosis and inflammation. *Genes Dev.* **27:**1640–1649; 2013.
[49] Cho, Y. S.; Challa, S.; Moquin, D.; Genga, R.; Ray, T. D.; Guildford, M.; Chan, F. K. Phosphorylation-driven assembly of the RIP1-RIP3 complex regulates programmed necrosis and virus-induced inflammation. *Cell* **137:**1112–1123; 2009.
[50] Torriglia, A.; Perani, P.; Brossas, J. Y.; Chaudun, E.; Treton, J.; Courtois, Y.; Counis, M. F. L-DNase II, a molecule that links proteases and endonucleases in apoptosis, derives from the ubiquitous serpin leukocyte elastase inhibitor. *Mol. Cell. Biol.* **18:**3612–3619; 1998.
[51] Altairac, S.; Zeggai, S.; Perani, P.; Courtois, Y.; Torriglia, A. Apoptosis induced by Na+/H+ antiport inhibition activates the LEI/L-DNase II pathway. *Cell Death Differ.* **10:**548–557; 2003.
[52] Moubarak, R. S.; Yuste, V. J.; Artus, C.; Bouharrour, A.; Greer, P. A.; Menissier-de Murcia, J.; Susin, S. A. Sequential activation of poly(ADP-ribose) polymerase 1, calpains, and Bax is essential in apoptosis-inducing factor-mediated programmed necrosis. *Mol. Cell. Biol.* **27:**4844–4862; 2007.
[53] Norberg, E.; Gogvadze, V.; Ott, M.; Horn, M.; Uhlen, P.; Orrenius, S.; Zhivotovsky, B. An increase in intracellular Ca^{2+} is required for the activation of mitochondrial calpain to release AIF during cell death. *Cell Death Differ.* **15:**1857–1864; 2008.
[54] Villalpando Rodriguez, G. E.; Torriglia, A. Calpain 1 induce lysosomal permeabilization by cleavage of lysosomal associated membrane protein 2. *Biochim. Biophys. Acta* **1833:**2244–2253; 2013.
[55] Baritaud, M.; Cabon, L.; Delavallee, L.; Galan-Malo, P.; Gilles, M. E.; Brunelle-Navas, M. N.; Susin, S. A. AIF-mediated caspase-independent necroptosis requires ATM and DNA-PK-induced histone H2AX Ser139 phosphorylation. *Cell Death Dis.* **3:**e390; 2012.
[56] Vanden Berghe, T.; Vanlangenakker, N.; Parthoens, E.; Deckers, W.; Devos, M.; Festjens, N.; Guerin, C. J.; Brunk, U. T.; Declercq, W.; Vandenabeele, P. Necroptosis, necrosis and secondary necrosis converge on similar cellular disintegration features. *Cell Death Differ.* **17:**922–930; 2010.
[57] Rubartelli, A.; Lotze, M. T. Inside, outside, upside down: damage-associated molecular-pattern molecules (DAMPs) and redox. *Trends Immunol.* **28:**429–436; 2007.
[58] Shang, Y. M.; Wang, G. S.; Sliney, D.; Yang, C. H.; Lee, L. L. White light-emitting diodes (LEDs) at domestic lighting levels and retinal injury in a rat model. *Environ. Health Perspect.* **122:**269–276; 2014.
[59] Jaadane, I.; Chahory, S.; Lepretre, C.; Omri, B.; Jonet, L.; Behar-Cohen, F.; Crisanti, P.; Torriglia, A. The activation of the atypical PKC zeta in light-induced retinal degeneration and its involvement in L-DNase II control. *J Cell Mol Med* ; 2015.